

Mechanically tunable magnetic properties of Fe₈₁Ga₁₉ films grown on flexible substrates

Guohong Dai, Qingfeng Zhan, Yiwei Liu, Huali Yang, Xiaoshan Zhang, Bin Chen, and Run-Wei Li

Citation: *Applied Physics Letters* **100**, 122407 (2012); doi: 10.1063/1.3696887

View online: <http://dx.doi.org/10.1063/1.3696887>

View Table of Contents: <http://scitation.aip.org/content/aip/journal/apl/100/12?ver=pdfcov>

Published by the *AIP Publishing*

Articles you may be interested in

[Static and high frequency magnetic properties of FeGa thin films deposited on convex flexible substrates](#)
Appl. Phys. Lett. **106**, 162405 (2015); 10.1063/1.4918964

[Magneto-elastic and magnetic domain properties of Fe₈₁Ga₁₉/Si\(100\) films](#)
J. Appl. Phys. **115**, 013909 (2014); 10.1063/1.4861160

[Controllable strain-induced uniaxial anisotropy of Fe₈₁Ga₁₉ films deposited on flexible bowed-substrates](#)
J. Appl. Phys. **114**, 173913 (2013); 10.1063/1.4829670

[Effect of buffer layer and external stress on magnetic properties of flexible FeGa films](#)
J. Appl. Phys. **113**, 17A901 (2013); 10.1063/1.4793602

[Effect of mechanical strain on magnetic properties of flexible exchange biased FeGa/IrMn heterostructures](#)
Appl. Phys. Lett. **102**, 022412 (2013); 10.1063/1.4776661

The logo for AIP APL Photonics is displayed in a white font on a red background. The letters 'AIP' are large and bold, followed by a vertical bar and the words 'APL Photonics' in a smaller font.

AIP | APL Photonics

APL Photonics is pleased to announce
Benjamin Eggleton as its Editor-in-Chief



Mechanically tunable magnetic properties of Fe₈₁Ga₁₉ films grown on flexible substrates

Guohong Dai,^{1,2,3} Qingfeng Zhan,^{1,2,a)} Yiwei Liu,^{1,2} Huali Yang,^{1,2} Xiaoshan Zhang,^{1,2} Bin Chen,^{1,2} and Run-Wei Li^{1,2,b)}

¹Key Laboratory of Magnetic Materials and Devices, Ningbo Institute of Material Technology and Engineering, Chinese Academy of Sciences, Ningbo 315201, People's Republic of China

²Zhejiang Province Key Laboratory of Magnetic Materials and Application Technology, Ningbo Institute of Material Technology and Engineering, Chinese Academy of Sciences, Ningbo 315201, People's Republic of China

³School of Science, Nanchang University, Nanchang 330031, People's Republic of China

(Received 20 January 2012; accepted 5 March 2012; published online 21 March 2012)

We investigated on magnetic properties of magnetostrictive Fe₈₁Ga₁₉ films grown on flexible polyethylene terephthalate (PET) substrates under various mechanical strains. The unstrained Fe₈₁Ga₁₉ films exhibit a significant uniaxial magnetic anisotropy due to a residual stress in PET substrates. It was found that the squareness of hysteresis loops can be tuned by an application of strains, inward/compressive or outward/tensile bending of the films. A modified Stoner-Wohlfarth model with considering a distribution of easy axes in polycrystalline films was developed to account for the mechanically tunable magnetic properties in flexible Fe₈₁Ga₁₉ films. These results provide an alternative way to tune mechanically magnetic properties, which is particularly important for developing flexible magnetoelectronic devices. © 2012 American Institute of Physics. [<http://dx.doi.org/10.1063/1.3696887>]

FeGa magnetostrictive alloys exhibit moderate magnetostriction (~ 350 ppm for Ga content of 19%) under very a low magnetic field (~ 100 Oe) but good mechanical properties.¹ Due to the great promise as engineering materials for applications in sensors and actuators, the magnetomechanical characteristics of FeGa alloys, including the magnetization and magnetostrictive responses to magnetic fields have been extensively investigated under applied tensile or compressive stresses.²⁻⁴ If the excellent magnetomechanical behaviors of magnetostrictive alloys can be achieved in thin films, they are possibly applied in magnetic microelectromechanical systems, and also important for developing functional materials, i.e., layered multiferroic composites.^{5,6} Most of previously studied magnetostrictive thin films and spintronic devices are deposited on stiff and thick substrates. Due to the significant clamping effect caused by substrates, when magnetostrictive films applied in micro-force sensors and multiferroic composited materials, their key performances, such as the strain sensitivity and the magnetoelectric coupling, are strongly dependence on the magnetomechanical behaviors of magnetostrictive layers, and therefore are drastically reduced.^{7,8} Recently, flexible magnetic films and spintronic devices grown on plastic substrates which can be shaped into almost any arbitrary geometry have attracted much attentions.^{9,10} The deformability of substrates may partially eliminate the substrate clamping and enhance the response of magnetostrictive films to external mechanical stress.^{11,12} So far, only few works systematically studied the stress dependence of the hysteresis loop properties for magnetic films and heterostructures.^{13,14} The magnetomechanical behaviors of magnetostrictive FeGa films especially grown

on flexible plastic substrates are not well known. Here, we fabricated magnetostrictive FeGa films on flexible polyethylene terephthalate (PET) substrates. Due to the residual stress of the flexible substrates, a uniaxial magnetic anisotropy is observed in the as-grown FeGa films. The magnetic properties can be significantly tuned with the application of strain by directly inward/compressive or outward/tensile bending of the films. Taking into account the distribution of the uniaxial anisotropy, the mechanically tunable magnetic behaviors can be qualitatively interpreted by a modified Stoner-Wohlfarth model.

Fe₈₁Ga₁₉ films with a thickness of 150 nm were deposited on both PET and Si substrates by radio frequency magnetron sputtering at room temperature. Before the substrates were transferred into the sputtering chamber, they were cleaned in ethyl alcohol using ultrasonic agitation for 15 min. The base pressure of the sputtering chamber was below 6.0×10^{-5} Pa. During deposition, the argon flow was kept at 50 sccm and the pressure was set at 1.0 Pa. An evaporation rate of 2.0 nm/min was used for the growth of Fe₈₁Ga₁₉ alloy. Prior to be taken out of the vacuum chamber, Fe₈₁Ga₁₉ films were capped by a 5 nm Au layer to avoid oxidation. The surface morphology of the films was characterized by atomic force microscopy (AFM) using Veco Dimension 3100 V. The angular dependence of hysteresis loops was measured using vibrating sample magnetometer (VSM, Lakeshore 7410) at room temperature.

Figures 1(a) and 1(b) show the AFM patterns for a bare PET substrate and Fe₈₁Ga₁₉/PET film, respectively. The root mean square (RMS) roughness of 2.16 nm for the PET substrate is much larger than that of 0.60 nm for the thermally oxidized Si substrate. For the fabrication of flexible magnetoelectronic devices, the surface roughness of the flexible substrate is required to decrease to a low value close to that

^{a)}Electronic mail: zhanqf@nimte.ac.cn.

^{b)}Electronic mail: runweili@nimte.ac.cn.

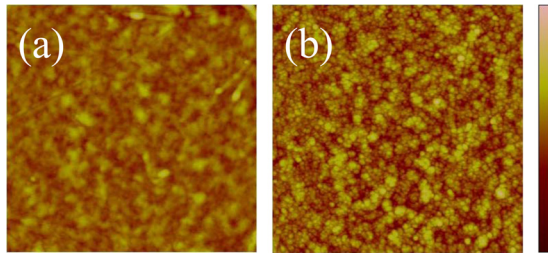


FIG. 1. AFM images ($2 \times 2 \mu\text{m}^2$) for (a) a flexible PET substrate and (b) an Fe₈₁Ga₁₉/PET film. The color contrast (dark to bright) for the height scale corresponds to 40 nm.

of Si wafers by means of spin-coating a photoresist buffer layer onto the plastic substrates.⁹ In our works, Fe₈₁Ga₁₉ layers are directly grown on PET substrates, the corresponding AFM image confirms the growth of polycrystalline Fe₈₁Ga₁₉ films with an RMS roughness of 3.34 nm. Due to the rough morphology of both PET substrates and Fe₈₁Ga₁₉ films, the coercive field of the as-grown Fe₈₁Ga₁₉/PET films is obviously larger than that of the reference samples grown on oxidized Si substrates.

In order to study the magnetic properties of Fe₈₁Ga₁₉/PET films at unstressed state, the hysteresis loops were measured at room temperature with a magnetic field applied parallel to the film plane. The field orientation φ is varied from 0° to 360° by rotating the sample with an increment of 10° , as shown in the inset of Fig. 2(a). The hysteresis loop for the field applied along the easy axis, i.e., $\varphi = 0^\circ$, is relative square with a M_r/M_s ratio of 0.86, while the hysteresis loop along the hard axis, i.e., $\varphi = 90^\circ$, is sheared with a squareness of 0.37, as shown in Fig. 2(a). The squareness and coercivity as a function of φ are illustrated in Fig. 2(b). Both of them possess a uniaxial symmetry about the easy or hard axes of Fe₈₁Ga₁₉/PET films, which indicates a significant uniaxial magnetic anisotropy, but not the magnetocrystalline anisotropy in Fe₈₁Ga₁₉/PET films due to the polycrystalline structure. In contrast, the uniaxial anisotropy for the reference samples grown on oxidized Si substrates is too weak to be observed. Therefore, we ascribe the uniaxial anisotropy of the flexible Fe₈₁Ga₁₉ films to the residual stress caused by the slightly inevitable deformation of PET substrates. Due to the adhesion of both mechanical interlocking and chemical bonding between Fe₈₁Ga₁₉ films and PET substrates, the residual stress and the applied stress could be

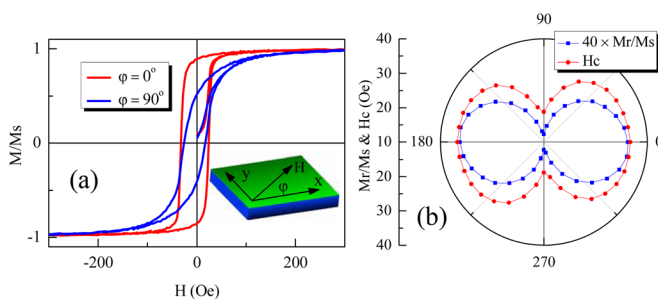


FIG. 2. (a) Hysteresis loops and initial magnetization curves for flexible Fe₈₁Ga₁₉/PET films with a magnetic field applied along the easy axis ($\varphi = 0^\circ$) and the hard axis ($\varphi = 90^\circ$). (b) Squareness and coercive field as a function of the field orientation φ for Fe₈₁Ga₁₉/PET exhibit a uniaxial symmetry about the easy or hard axes. The field orientation φ is defined in the inset of (a).

effectively transferred from flexible substrates to magnetostrictive films.¹⁵ The strength of the induced uniaxial anisotropy, K_u , is quantitatively evaluated by calculating the difference between works done in magnetization along different directions. Using the relation $K_u = \frac{1}{V} (\int_0^{M_s} H dM - \int_0^{M_s} H dM)$ and the initial M - H curves along both the easy and hard axes shown in Fig. 2(a), K_u is obtained to be $1.81 \times 10^5 \text{ erg/cm}^3$, which is comparable to the magnetocrystalline anisotropy of Fe₈₁Ga₁₉.¹⁶

Due to the inverse magnetostrictive effect, i.e., the Villari effect, the magnetic properties of the magnetostrictive materials is sensitive to the external mechanical stress. Thanks to the deformability of PET substrates, the compressive and tensile strains can be applied on Fe₈₁Ga₁₉ films by inward or outward bending the PET substrates. The hysteresis loops for Fe₈₁Ga₁₉/PET films under various strains are measured by slightly bending the substrates along the easy or hard axes of Fe₈₁Ga₁₉ films. In order to restrict the magnetic field parallel to the film plane, during the VSM measurement, the magnetic field, H , is applied perpendicular to the bending direction, i.e., the bending strain, as shown in the inset of Fig. 3. The strain, ε , and the stress, σ , are evaluated by using the relations $\varepsilon = t/2\rho$ and $\sigma = \varepsilon E_f/(1 - \nu^2)$, respectively, where t is the thickness of the substrate including the film thickness, ρ is the curvature radius of the substrate after bending, E_f is Young's modulus, and ν is the Poisson ratio. ε and σ are considered to be positive for the outward/tensile bending and negative for the inward/compressive bending. During the magnetic measurements, ε is applied within a maximum value of 0.78%, which corresponds to $\sigma = 0.51 \text{ GPa}$ by using $E_f = 60 \text{ GPa}$ for Fe₈₁Ga₁₉ and the typical value of $\nu = 0.3$ for metals.^{4,17} When the magnetic field is applied along the easy axis of the films, a tensile strain along the hard axis increasing from 0% to 0.78% gives rise to a drastic decrease in M_r/M_s ratio from 0.86 to 0.29, as shown in Fig. 3(a). In contrast, under a compressive strain of -0.26% , the M_r/M_s ratio is increased to 0.89. With further increasing the compressive strain, both the squareness and coercivity become hard to be improved, as shown in Fig. 3(b). For the magnetic field oriented along the hard axis, the M_r/M_s ratio can be tuned from 0.37 at an unstressed state to 0.19 under a tensile strain of 0.78% and to 0.79 under a compressive strain of -0.78% applied along the easy axis, as shown in Figs. 3(c) and 3(d), respectively. The external strain dependence of squareness is summarized in Fig. 4(a). For our measurement configurations, the tensile strain leads to a decrease in M_r/M_s ratio, but the compressive strain increases this value. It should be noted that, considering the contribution on the magnetoelastic energy and the induced magnetic anisotropy, the effect of a tensile strain applied along the easy axis is equivalent to that of a compressive strain along the hard axis and vice versa. Our results suggest that the easy axis for a flexible magnetostrictive film can be tuned to the hard axis under a tensile strain applied along the hard axis or a compressive strain along the easy axis, meanwhile the hard axis of the films is changed to the easy axis. In addition, we have prepared Fe₈₁Ga₁₉/PET films with various thicknesses down to 10 nm. They exhibit the similar residual stress-induced uniaxial anisotropy and the similar mechanically tunable magnetic properties.

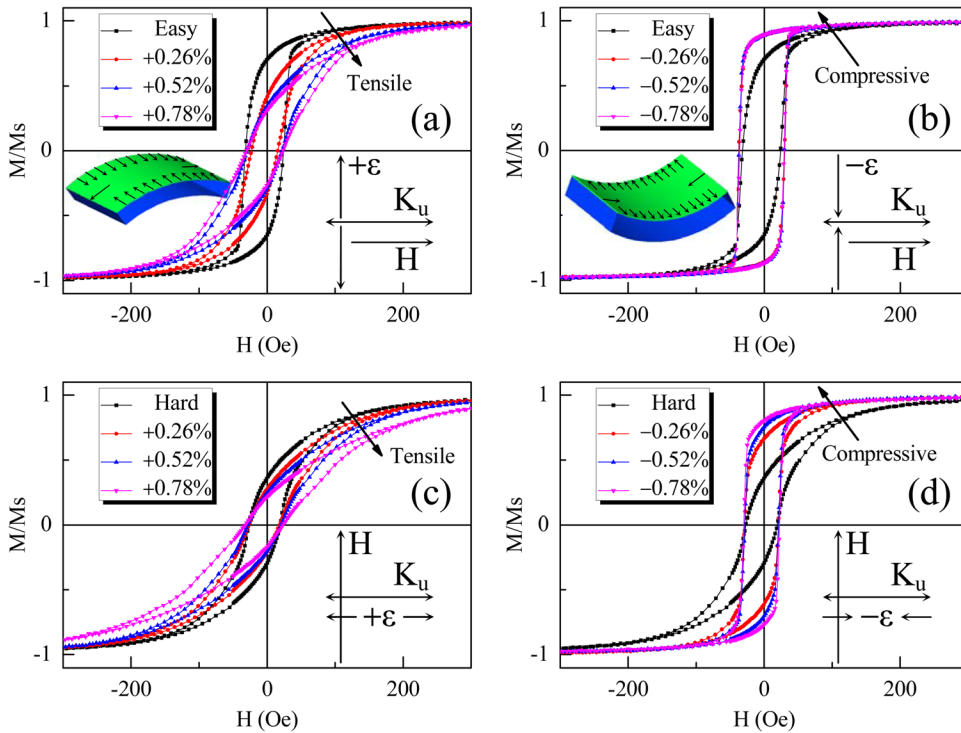


FIG. 3. Hysteresis loops for $\text{Fe}_{81}\text{Ga}_{19}/\text{PET}$ obtained under various external strains using different measuring configurations, (a) Magnetic field H parallel to the uniaxial anisotropy K_u and a tensile strain $+\varepsilon$ (outward bending of PET substrates) applied perpendicular to K_u , (b) H parallel to K_u and a compressive strain $-\varepsilon$ (inward bending) perpendicular to K_u , (c) H perpendicular to K_u and $+\varepsilon$ parallel to K_u , and (d) H perpendicular to K_u and $-\varepsilon$ parallel to K_u .

We intuitively ascribe the mechanically tunable M_r/M_s ratio to an additional uniaxial anisotropy induced by the various external strains. In our experiments, the strain is either along the easy axis or along the hard axis of $\text{Fe}_{81}\text{Ga}_{19}$ films, that is, the external strain-induced uniaxial anisotropy, K_e , is collinear or perpendicular to K_u . We consider such a system with a uniaxial anisotropy of $K_u/M_s = 120$ Oe which is close to the experimental observation for our $\text{Fe}_{81}\text{Ga}_{19}$ films. The tensile stress $+\sigma$ and the compressive stress $-\sigma$, which are applied perpendicular to the easy axis of K_u , give rise to a positive K_e with the easy axis perpendicular to K_u and a negative K_e with the easy axis along K_u , respectively, as schematically shown in the inset of Fig. 4(b). Regardless of the strength of K_e , the hysteresis loop predicted by Stoner-

Wohlfarth model¹⁸ for $\varphi = 0^\circ$ or $\varphi = 90^\circ$ is either a perfect rectangle with a squareness of one along the easy axis or a sheared one with the remanence of zero along the hard axis. The squareness switched between 1 and 0, i.e., the easy axis changed to the hard axis or vice versa, occurs at $K_e = K_u$, as shown in Fig. 4(b). As a result, based on the magnetization reversal mechanism of coherent rotation, we cannot theoretically draw the conclusion that the external stresses applied along or perpendicular to K_u could tune the squareness of hysteresis loops for magnetostrictive films.

For the as-grown $\text{Fe}_{81}\text{Ga}_{19}$ films, we notice that the squareness of the hysteresis loop is less than one along the easy axis but higher than zero along the hard axis [see Fig. 2(a)]. The experimental observation indicates that our

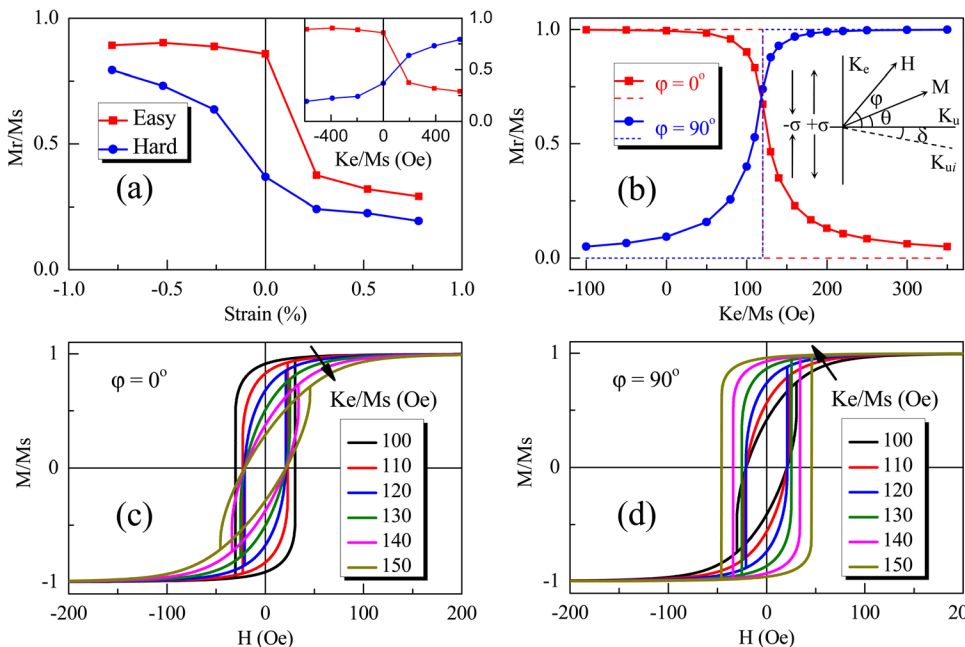


FIG. 4. (a) Summary for the strain dependence of squareness with the magnetic field applied along the easy and hard axes. (b) Calculated squareness of hysteresis loops as a function of the strain-induced uniaxial anisotropy K_e/M_s using the Stoner-Wohlfarth model (dashed lines) and our modified one (solid lines with symbols). Calculated hysteresis loops under various K_e/M_s for the magnetic field (c) parallel and (d) perpendicular to K_u . The magnetic field and anisotropy geometries used for numerical calculations are shown in the inset of (b). Using this definition, the experimental results can be accordingly revised to the squareness as a function of K_e/M_s , as plotted in the inset of (a).

samples are essentially not a perfect uniaxial system. Therefore, it is reasonable to speculate that the uniaxial anisotropy for the grains in polycrystalline $\text{Fe}_{81}\text{Ga}_{19}$ films does not strictly orient in an identical direction, but has a distribution along its average direction, that is, K_u . Considering an arbitrary grain with a uniaxial anisotropy, K_{ui} , orienting at an angle of δ with respect to the orientation of K_u , an external stress σ is applied perpendicular to K_u . Thus, the total energy for a grain in $\text{Fe}_{81}\text{Ga}_{19}$ films can be written as: $E = -K_{ui}\cos^2(\theta - \delta) + K_e\cos^2\theta - \text{MH}\cos(\theta - \varphi)$, where θ is the angle between K_u and the magnetization vector M . We assume that the anisotropy constant K_{ui} for each grain is identical to K_u , and the angle of δ for the distribution of K_{ui} is ranged from -10° to 10° with respect to K_u . Due to the distribution of the easy axis, the average value K_u for the whole film is only less than K_{ui} about one percent, which can be neglected in our numerical calculations. Using an intermediate value of $\delta = 5^\circ$, we obtain the hysteresis loops predicted under various K_e by means of Stoner-Wohlfarth model. As shown in Fig. 4(c), the simulated hysteresis loops for H along the easy axis of K_u , i.e., $\varphi = 0^\circ$, indicate that when K_e/M_s caused by a tensile stress is varied from 100 to 150 Oe, the squareness can be obviously reduced from 0.91 to 0.29 and the coercivity is slightly decreased from 30 to 21 Oe. For H along the hard axis of K_u , i.e., $\varphi = 90^\circ$, the squareness of the hysteresis loops is enhanced from 0.41 to 0.96, and the coercivity is increased from 21 to 46 Oe, as shown in Fig. 4(d). We calculated the K_e/M_s dependence of squareness for δ distributed from -10° to 10° , the average values are displayed in Fig. 4(b). With increasing K_e/M_s , i.e., σ , the squareness is drastically decreased for $\varphi = 0^\circ$ and is increased for $\varphi = 90^\circ$, especially around the critical value of $K_e = K_u$, where K_u is compensated by K_e . Our numerical calculations are in good agreement with the simulations done in Ni films using a micromagnetic model including the magnetoelastic energy term into the Landau-Lifshitz-Gilbert equation.¹⁹ It should be noted that to facilitate the simulations and discussions, we utilize the uniform anisotropy geometry for our calculations, which is different from the experimental configurations. In experiment, the strain of substrates bending changes the magnetoelastic energy of the films, producing an equivalent uniaxial anisotropy K_e . Employing the definition for simulation shown in the inset of Fig. 4(b), the strength of K_e can be written as $K_e = -3/2\lambda\sigma$, where λ is the magnetostriction constant for polycrystalline $\text{Fe}_{81}\text{Ga}_{19}$ films. Using $\lambda = 100$ ppm,¹² the experimental strain dependence of squareness for $\text{Fe}_{81}\text{Ga}_{19}/\text{PET}$ films can be accordingly revised to the squareness as a function of K_e/M_s , as plotted in the inset of Fig. 4(a). Obviously, our simulations based on the modified Stoner-Wohlfarth model are able to nicely interpret the mechanically tunable squareness of hysteresis loops for $\text{Fe}_{81}\text{Ga}_{19}$ films. The discrepancy between our experimental results and simulations may arise from the uncertain coefficients used for calculations and also from the irreversible behaviors involving domain wall motion and incoherent rotation especially, while the magnetic field was applied around the easy axis.²⁰ The distribution of easy axes,

which likely come from the inhomogeneous residual stress in $\text{Fe}_{81}\text{Ga}_{19}$ films due to the flexible PET substrates, is the key factor for the occurrence of the experimental observations.

In summary, we fabricated magnetostrictive $\text{Fe}_{81}\text{Ga}_{19}$ films on flexible PET substrates, in which a significant uniaxial magnetic anisotropy is observed for the unstressed state. The hysteresis loops were measured under various compressive or tensile strains by inward or outward bending of the films. The M_r/M_s ratio is increased with the application of compressive strains and is decreased with the tensile strains applied along the easy or hard axis of $\text{Fe}_{81}\text{Ga}_{19}$ films. Consequently, the easy axis can be tuned to the hard axis or vice versa. Based on a modified Stoner-Wohlfarth model, in which the distribution of easy axes in polycrystalline films was considered, the mechanically tunable magnetic properties in flexible $\text{Fe}_{81}\text{Ga}_{19}$ films can be well understood.

The authors acknowledge the financial support from the National Natural Foundation of China (11174302), State Key Project of Fundamental Research of China (2012CB933004), Zhejiang and Ningbo Natural Science Foundations, Chinese Academy of Sciences (CAS), and Ningbo Science and Technology Innovation Team (2011B82004, 2009B21005).

- ¹A. E. Clark, J. B. Restorff, M. Wun-Fogle, T. A. Lograsso, and D. L. Schlager, *IEEE Trans. Magn.* **36**, 3238 (2000).
- ²J. Atulasimha and A. B. Flatau, *Smart Mater. Struct.* **20**, 043001 (2011).
- ³A. Mahadevan, P. G. Evans, and M. J. Dapino, *Appl. Phys. Lett.* **96**, 012502 (2010).
- ⁴R. A. Kellogg, A. B. Flatau, A. E. Clark, M. Wun-Fogle, and T. A. Lograsso, *J. Appl. Phys.* **91**, 7821 (2002).
- ⁵S. A. Wilson, R. P. J. Jourdain, Q. Zhang, R. A. Dorey, C. R. Bowen, M. Willander, Q. U. Wahab, M. Willander, S. M. Al-hilli, O. Nur et al., *Mater. Sci. Eng. R.* **56**, 1 (2007).
- ⁶W. Eerenstein, N. D. Mathur, and J. F. Scott, *Nature* **442**, 759 (2006).
- ⁷S. Dokupil, M.-T. Bootsmann, S. Stein, M. Löhndorf, and E. Quandt, *J. Magn. Magn. Mater.* **290–291**, 795 (2005).
- ⁸H. Zheng, J. Wang, S. E. Lofland, Z. Ma, L. Mohaddes-Ardabili, T. Zhao, L. Salamanca-Riba, S. R. Shinde, S. B. Ogale, F. Bai et al., *Science* **303**, 661 (2004).
- ⁹Y. F. Chen, Y. Mei, R. Kaltfen, J. I. Mönch, J. Schumann, J. Freudenberger, H.-J. Klaub, and O. G. Schmidt, *Adv. Mater.* **20**, 3224 (2008).
- ¹⁰C. Barraud, C. Deranlot, P. Seneor, R. Mattana, B. Dlubak, S. Fusil, K. Bouzehouane, D. Deneuve, F. Petroff, and A. Fert, *Appl. Phys. Lett.* **96**, 072502 (2010).
- ¹¹S. F. Zhao, J. G. Wan, M. L. Yao, J. M. Liu, F. Q. Song, and G. H. Wang, *Appl. Phys. Lett.* **97**, 212902 (2010).
- ¹²T. Brintlinger, S. H. Lim, K. H. Baloch, P. Alexander, Y. Qi, J. Barry, J. Melngailis, L. Salamanca-Riba, I. Takeuchi, and J. Cumings, *Nano Lett.* **10**, 1219 (2010).
- ¹³L. Callegaro and E. Puppini, *Appl. Phys. Lett.* **68**, 1279 (1996).
- ¹⁴D. H. Han, J. G. Zhu, J. H. Judy, and J. M. Sivertsen, *J. Appl. Phys.* **81**, 4519 (1997).
- ¹⁵V. K. Khanna, *J. Phys. D: Appl. Phys.* **44**, 034004 (2011).
- ¹⁶S. Rafique, J. R. Cullen, M. Wuttig, and J. Cui, *J. Appl. Phys.* **95**, 6939 (2004).
- ¹⁷N. Lei, S. Park, P. Lecoeur, D. Ravelosona, C. Chappert, O. Stelmakovich, and V. Holy, *Phys. Rev. B* **84**, 012404 (2011).
- ¹⁸E. C. Stoner and E. P. Wohlfarth, *Philos. Trans. R. Soc. London, Ser. A* **240**, 599 (1948).
- ¹⁹B. Zhu, C. C. H. Lo, S. J. Lee, and D. C. Jiles, *J. Appl. Phys.* **89**, 7009 (2001).
- ²⁰J. Camarero, J. Sort, A. Hoffmann, J. M. García-Martín, B. Dieny, R. Miranda, and J. Nogués, *Phys. Rev. Lett.* **95**, 057204 (2005).